ELEKTROTEHNIŠKI VESTNIK 88(1-2): 26-32, 2021
ORIGINAL SCIENTIFIC PAPER

Improved IM DTC by using a Fuzzy Switching Table in PV Applications

Sofia Lalouni Belaid

Laboratoire de Technologie Industrielle et de l'Information(LTII), Faculté de Technologie, Université de Bejaia, 06000 Bejaia Algérie
E-mail: lalouni_sofia@yahoo.fr

Abstract. The paper proposes a fuzzy inference system to improve the direct torque control (FDTC) of the induction motor (IM) using a photovoltaic (PV) water pumping system. The large ripples in the conventional control (CDTC) are due to the control action, based on hysteresis comparators, that doesn't take into account the error level of the flux/torque. Using a fuzzy switching table, voltage vectors are selected according to the error range. A number of the sectors is increased in order to have more freedom degrees for the selection of the voltage source inverter switching vector. To extract the maximum available power from a PV generator, an intelligent controller based on a fuzzy logic is used. Results of a simulation made with MATLAB/SIMULINK show the effectiveness of the proposed FDTC in terms of an important reduction of the torque and flux ripples and THD of the stator current compared to CDTC.

Keywords: photovoltaic (PV) energy, pumping system, induction motor (IM), direct torque control (DTC); fuzzy direct torque control (FDTC);

Izboljšan način neposrednega nadzora navora z uporabo mehke preklopne tabele v fotonapetostnem sistemu

V prispevku je predstavljen sistem mehkega načina vodenja za izboljšanje neposrednega nadzora navora (DTC) v fotonapetostnem sistemu za črpanje vode na osnovi asinhronega motorja. Velika odstopanja, ugotovljena v običajnem DTC, so posledica krmilnega delovanja, temelječega na primerjalnikih s histerezo, ki ne upoštevajo stopnje napake navora. Z mehko preklopno tabelo smo izbrali napetostne vektorje glede na obseg napak. Večjo možnost pri izbiri preklopnih vektorjev smo dosegli s povečanjem števila sektorjev. Za dosego največje razpoložljive moči iz fotovoltaičnega vira smo uporabili inteligentni krmilnik, ki temelji na mehki logiki. Rezultati simulacij potrjujejo učinkovitost predlaganega mehkega načina vodenja v smislu pomembnega zmanjšanja odstopanja navora in pretoka v primerjavi s konvencionalnim načinom.

1 INTRODUCTION

Global energy demand continues to grow year after year, which encourages many investments in renewable energy solutions. Now, that there are many forms of the renewable energies, the most commonly used are the solar, wind and hydraulic energies [1]. Photovoltaic (PV) solar energy is favorited and an economic solution for several applications. It is clean, free, abundant and environmentally friendly. PV systems are used for pumping water to meet daily needs (human, agricultural and livestock). However, the PV system efficiency is still low. A maximum power point tracking (MPPT) control should be introduced to maximize the efficiency of the PV array. A lot of authors are interested in the PV system control strategies in order to improve its effectiveness [1,2].

For pumping applications, the induction motor (IM) is widely used because of its robustness, high efficiency, low cost and maintenance free [2-4]. Different control techniques have been reported in the literature in order to enhance the IM performance [3-15]. Several studies use direct or indirect field-oriented control (FOC) methods [3,5,13]. However, with those techniques, the system performance is affected by internal parameter variations as well as external disturbances.To overcome these disadvantages, IM DTC is proposed as a new technique [6-12,14-22]. It is characterized by its robustness and high dynamic performance neither a PWM modulation block nor an inner current control loop used in classical FOC. DTC suffers from high torque and flux ripples caused by the hysteresis comparators that generate mechanical vibrations and disagreeable acoustic noise and, therefore, degrade the IM performance [7-9]. In [10-12, 14-16, 19,21, 22] several solutions were proposed by researchers to cope with these drawbacks. In [11], a predictive DTC control is proposed. However, to use this technique, the cost function for each voltage vector needs to be evaluated. In [12], a sliding mode control is used to improve DTC, but the chattering phenomenon is unavoidable. Some authors propose ripple reduction by using multilevel inverters [10, 14-16, 22], which increase the switching

Received 30 May 2020
Accepted 20 November 2020

losses and inverter cost. In [19,21] , an improvement is proposed using a space-vector-modulation-based DTC that requires the system parameters and controllers sizing which increases the system complexity.
Recently, a DTC improvement using intelligent control techniques has gained an increased attention [1,2,7-9, 14, 17,18, 20]. Fuzzy logic controllers (FLC) depend neither on the system parameters nor on the system mathematical models and are able to handle non linearity [7-9] . In the paper, Fuzzy DTC (FDTC) with twelve sectors is used to improve the PV pumping system performance. A Fuzzy switching table is introduced to cope with the drawbacks of the conventional DTC (CDTC). A Fuzzy-inference-system-based MPPT controler is adressed as a solution to the conventional MPPT methods. The simulation results prove that the Fuzzy MPPT controller has a very robust behavior and ensures fast and fine tracking througout the day. A comparison made between the two controllers shows that the proposed method significantly reduces the torque/flux ripple and the stotor current THD, thus improving performance enabling it to operate the PV pumping system with less mechanical IM vibrations, and acoustic noise.

2 PUMPING SYSTEM MODELING

2.1 PV array modeling

The PV generator is a series and/or a parallel combination of PV panels composed of several cells. It is modelled by of a photo-current source in parallel with a diode connected with series R_s and shunt R_{sh} resistors. The PV current is calculated using Eq.1 [1-3]:

$$I_{pv} = I_{ph} - I_0\left(\exp\left[\frac{q\left(V + R_s I_{pv}\right)}{N_s AKT}\right] - 1\right) - \frac{\left(V + R_s I_{pv}\right)}{R_{sh}} \quad (1)$$

where, I_{ph} is the photo-current, I_0 is the diode saturation current, q is the electron charge (1.602×10^{-19} *C*), A is the ideality factor, K is the Boltzmann's constant (1.381×10^{-23} *J/K*), T is the temperature junction and N_s is the number of cells in a series. Fig.1 shows the 3D P_{pv}-I_{pv}-V_{pv} characteristic of the studied PV pannel for different levels of irradiation at a constant temperature (25°C).

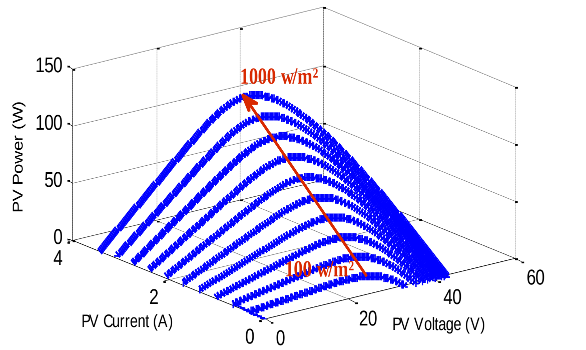

Figure 1. PV characteristics for different irradiation levels at 25°C.

2.2 Induction machine and pump modeling

The IM dynamic model in the α-β frame is given by Eq.2.

$$\begin{cases} V_{s\alpha} = R_s i_{s\alpha} + L_s \dfrac{di_{s\alpha}}{dt} + M\dfrac{di_{r\alpha}}{dt} \\ V_{s\beta} = R_s i_{s\beta} + L_s \dfrac{di_{s\beta}}{dt} + M\dfrac{di_{r\beta}}{dt} \\ 0 = R_r i_{r\alpha} + L_r \dfrac{di_{r\alpha}}{dt} + M\dfrac{di_{s\alpha}}{dt} + \omega(M i_{s\beta} + L_r i_{r\beta}) \\ 0 = R_r i_{r\beta} + L_r \dfrac{di_{r\beta}}{dt} + M\dfrac{di_{s\beta}}{dt} - \omega(M i_{s\alpha} + L_r i_{r\alpha}) \end{cases} \quad (2)$$

Where $V_{s\alpha}$, $V_{s\beta}$, $i_{s\alpha}$, $i_{s\beta}$, $i_{r\alpha}$, $i_{r\beta}$ are α-β components of the stator/rotor voltage and current respectively, Ω is the machine speed (pΩ=ω), R_s, R_r, L_s, L_r, M are the stator/rotor phase resistances, inductances, mutual inductance respectively.

The Pleider-Peterman's model is used. It provides the centrifugal pump curves, and its parameters are the speed (*Ω*) and the flow (*Q*). It is identified by Eq.3, where coefficients C_1, C_2 and C_3 are the functions of the pump characteristics (shape and dimensions of the vanes and diffuser) given by the manufacturer [13].The maometric head (H_M) follows, is calculated as follow:

$$H_M = C_1\Omega^2 - C_2\Omega Q - C_3\Omega^2 \quad (3)$$

The hydraulic power is a function on the water density (*ρ*) and gravity (*g*), given by Eq.4.

$$P_H = \rho\, g\, H_M\, Q \quad (4)$$

The centrifugal pump opposes the resistive torque (T_r) which depends on the pump nominal power and speed.

$$T_r = \left(\frac{P_n}{\Omega_n^3}\right)\Omega^2 + T_s \quad (5)$$

2.3 MPPT control

The main task of the MPPT control is to ensure a continuous tracking of the maximum power point of a PV system. Due to the high non-linearity of the I_{pv}-V_{pv} and P_{pv}-V_{pv} characteristic of PV pannel (Fig.1), such MPPT control is indispensable to guaranty the

Table 1. Fuzzy MPPT controller rule table [23]

ΔV_{pv}/ ΔP_{pv}	BN	MN	SN	Z	SP	MP	BP
BN	BP	BP	MP	Z	MN	BN	BN
MN	BP	MP	SP	Z	SN	MN	BN
SN	MP	SP	SP	Z	SN	SN	MN
Z	BN	MN	SN	Z	SP	MP	BP
SP	MN	SN	SN	Z	SP	SP	MP
MP	BN	MN	SN	Z	SP	MP	BP
BP	BN	BN	MN	Z	MP	BP	BP

deliverance of the available maximum power under uniform or varying atmospheric conditions.

Over the years, many MPPT algorithms have been reported in the literature [1-4, 23, 24].These are, a fractional method, perturb and observe (P&O) and incremental conductance (INC) (using a constant or variable step) and heuristic methods (fuzzy logic, genetic algorithms and neural network). These methods differ difference in the speed of convergence, degree of difficulty and cost. In the paper MPPT based on FLC is used for being simple to understand, able to manage the nonlinearity problem, suitable for complex models and inexpensive to develop [23]. FLC ensures fast and fine tracking regardless of atmospheric variations compared to the P&O methods (Fig. 2). Table .1 shows the rule table.

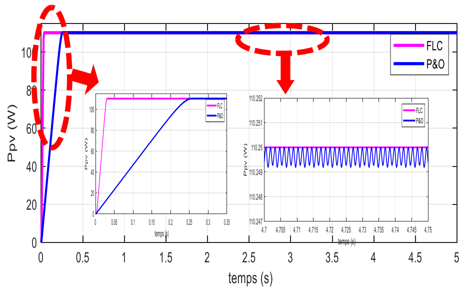

Figure 2. Photovoltaic power waveform with zoom.

3 CONVENTIONAL DIRECT TORQUE CONTROL (CDTC)

The CDTC strategy was first introduced in the mid '80s for the IM control [11]. It is characterized by its robustness and good dynamic performance needing, neither PWM modulation block nor an inner current control loop used in classical FOC. The stator voltage vector is selected with a look-up table according to the difference between the reference and the estimated motor electromagnetic (EM) torque and rotor flux. This difference is digitalized using a three and two-level hysteresis comparator and applied as an input with a flux angle to a switching table (Table. 2)[7-9]. The stator-flux vector is estimated from the IM voltage and current measurements along the α and β axes [7-9]. The EM torque is estimated using Eq.11.
The stator currents in the stationary reference frame (α,β) are calculated as follow:

$$\begin{cases} i_{s\alpha} = \sqrt{\dfrac{2}{3}} i_{sa} \\ i_{s\beta} = \dfrac{1}{\sqrt{2}}(i_{sb} - i_{sc}) \end{cases} \quad (6)$$

Using the DC voltage and the inverter switching states, the α and β components of the stator voltage are calculated according to Eq.7 [4]:

$$\begin{cases} v_{s\alpha} = \sqrt{\dfrac{2}{3}} V_{dc}(S_a - \dfrac{S_b + S_c}{2}) \\ v_{s\beta} = \sqrt{\dfrac{1}{2}} V_{dc}(S_b - S_c) \end{cases} \quad (7)$$

The magnitude of the stator flux is calculated with Eq.8:

$$\varphi_s = \sqrt{\varphi_{s\alpha}^2 + \varphi_{s\beta}^2} \quad (8)$$

where the stator flux is estimated according to Eq.9.

$$\begin{cases} \varphi_{s\alpha} = \int_0^t (v_{s\alpha} - R_s . i_{s_\alpha})dt \\ \varphi_{s\beta} = \int_0^t (v_{s\beta} - R_s . i_{s_\beta})dt \end{cases} \quad (9)$$

The stator-flux space is divided into six sectors.

Its angle (θ_s) is calculated using Eq.10 [8]:

Table 2. The switching table of CDTC [9]

θs		θ1	θ2	θ3	θ4	θ5	θ6
Δφs	**ΔTe**						
1	1	V_2	V_3	V_4	V_5	V_6	V_1
	0	V_7	V_0	V_7	V_0	V_7	V_0
	-1	V_6	V_1	V_2	V_4	V_4	V_5
0	1	V_3	V_4	V_5	V_6	V_1	V_2
	0	V_0	V_7	V_0	V_7	V_0	V_7
	-1	V_5	V_6	V_1	V_2	V_3	V_4

$$\theta_s = \tan^{-1}(\frac{\varphi_{s\beta}}{\varphi_{s\alpha}}) \quad (10)$$

The EM torque is estimated using Eq.11.

$$T = p(\varphi_{s\alpha} . i_{s\beta} - \varphi_{s\beta} . i_{s\alpha}) \quad (11)$$

4 FUZZY FDTC

To overcome the drawback of the CDTC, i.e high flux ripples and torque, the hysteresis comparators and look-up table are replaced by a fuzzy logic inference system. The improvement using a fuzzy logic is due to the controller, non-dependence on the system parameters or complex mathematical model and its handling the non-linearity [7] .
The large ripples in CDTC are due to the invariable control action irrespective of the error size. So using the proposed fuzzy system we introduce a notion of a large or small error and applies different voltage vectors for each of them [8, 16-18]. The increase in the number of the sectors helps taking an appropriate decision in termes of the voltage vectors. The generated switching vector is based on the level of the flux and torque error size and the sectors number. To improve the PV water pumping system performance and to minimize the stator

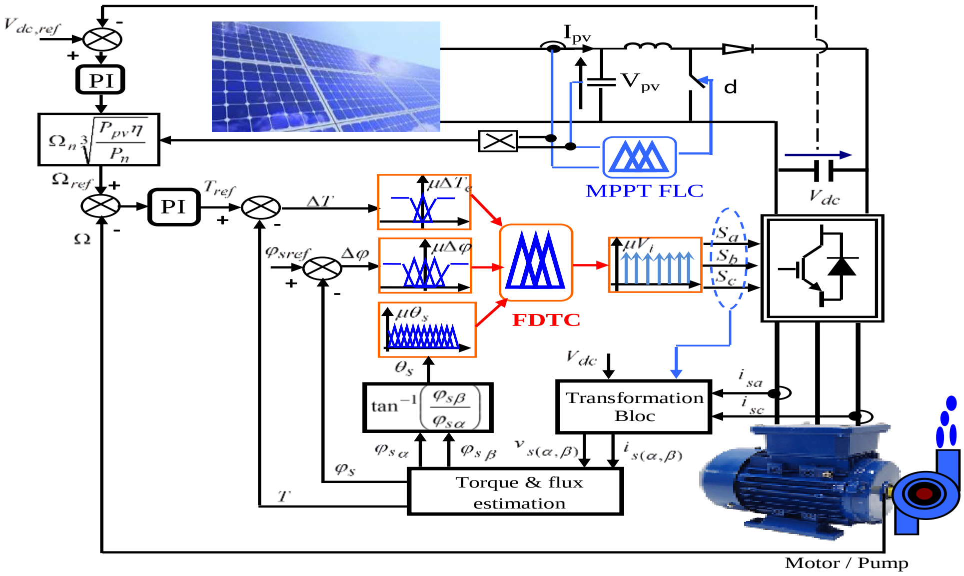

Figure 3. Block diagram of PV pumping system with fuzzy direct torque control.

Table 3. Fuzzy rule base of FDTC [7]

ΔT	Δφ \ θ	θ1	θ2	θ3	θ4	θ5	θ6	θ7	θ8	θ9	θ10	θ11	θ12
PL	**P**	V_1	V_2	V_2	V_3	V_3	V_4	V_4	V_5	V_5	V_6	V_6	V_1
	Z	V_2	V_2	V_3	V_3	V_4	V_4	V_5	V_5	V_6	V_6	V_1	V_1
	N	V_2	V_3	V_3	V_4	V_4	V_5	V_5	V_6	V_6	V_1	V_1	V_2
PS	**P**	V_1	V_2	V_2	V_3	V_3	V_4	V_4	V_5	V_5	V_6	V_6	V_1
	Z	V_2	V_3	V_3	V_4	V_4	V_5	V_5	V_6	V_6	V_1	V_1	V_2
	N	V_3	V_3	V_4	V_4	V_5	V_5	V_6	V_6	V_1	V_1	V_2	V_2
ZE	**P**	V_0	V_0	V_0	V_0	V_0	V_0	V_0	V_0	V_0	V_0	V_0	V_0
	Z	V_0	V_0	V_0	V_0	V_0	V_0	V_0	V_0	V_0	V_0	V_0	V_0
	N	V_0	V_0	V_0	V_0	V_0	V_0	V_0	V_0	V_0	V_0	V_0	V_0
NS	**P**	V_6	V_6	V_1	V_1	V_2	V_2	V_3	V_3	V_4	V_4	V_5	V_5
	Z	V_0	V_0	V_0	V_0	V_0	V_0	V_0	V_0	V_0	V_0	V_0	V_0
	N	V_4	V_5	V_5	V_6	V_6	V_1	V_1	V_2	V_2	V_3	V_3	V_4
NL	**P**	V_6	V_6	V_1	V_1	V_2	V_2	V_3	V_3	V_4	V_4	V_5	V_5
	Z	V_5	V_6	V_6	V_1	V_1	V_2	V_2	V_3	V_3	V_4	V_4	V_5
	N	V_5	V_5	V_6	V_6	V_1	V_1	V_2	V_2	V_3	V_3	V_4	V_4

flux and EM torque ripples, the fuzzy controller produces an optimal voltage vector by calculating the optimal vector angle using instantaneous stator-flux and torque errors.

The fuzzy inputs are the torque and flux errors and the stator flux angle position (θ_s). The first input consists of three linguistic variables: positive (P), zero (Z) and negative (N). The torque error is minimized and divided into five linguistic variables: positive large (PL), positive small (PS), zero (Z), negative small (NS) and negative large (NL). The last input, (θ_s) is divided into twelve sectors making an appropriate voltage vector represented by 12 fuzzy sets (θ_1-θ_{12}). The sectors are determined by the Eq.11.

$$(n-2)\frac{\pi}{6} \langle\ \theta_n \ \langle\ (n-1)\frac{\pi}{6} \qquad (11)$$

where n is the number of the sectors, n=1,2 ,...,12.

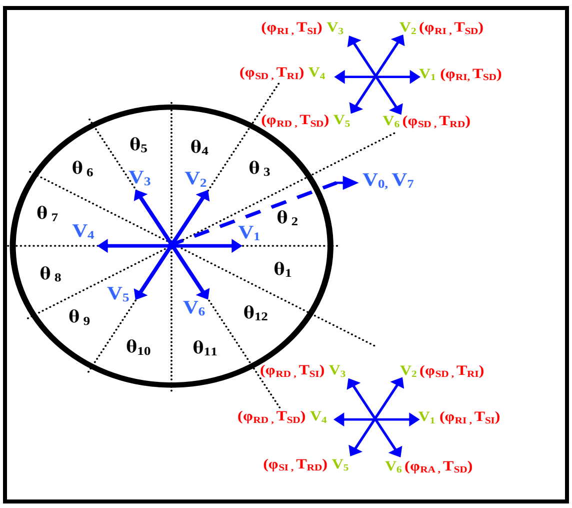

Figure 4. voltage vector selection for sectors 3 and 12, φ_{RI}/ φ_{RD}, φ_{SI}/ φ_{SD}, T_{RI}/ T_{RD}, T_{SI}/ T_{SD} are Flux/Torque with Rapid or Small, Increase/Decerase.

The fuzzy control rules are based on the min-max fuzzy inference system [7, 25]. An example can be formulated as follows:

IF (ΔT is PL) AND ($\Delta\varphi$ is P) AND (θ is θ_3) then $V=V_2$

This means, that the EM torque reference value is larger than the estimated value, the rotor flux reference is greater than the estimated one, and the sector θ_3 locate the rotor flux, this way a suitable voltage vector (V_2) is chosen that will slighty deacrese the EM torque and rapidly increase the rotor flux according to Fig. 4.

The rule table of the proposed strategy is shown in Table. 3. The inference method uses the Mamdani's procedure based on a min-max decision [2]. The defuzzification step transforms the output fuzzy results into numerical values representing one of the vectors (V_0-V_7). The membership function of the voltage vector output is written with Eqs.12, 13 and 14 [2, 25, 26].

$$\mu_{Vout}(V) = \max_{i=1}^{180}\left(\mu'_{Vi}(V)\right) \tag{12}$$

$$\mu'_{Vi}(V) = \max\left(\alpha_i, \mu_{Vi}(V)\right) \tag{13}$$

$$\alpha_i = \min\left(\mu_{Ai}(\Delta T), \mu_{Bi}(\Delta\varphi), \mu_{Ci}(\Delta\theta)\right) \tag{14}$$

where $\mu Ai(\Delta T)$, $\mu Bi(\Delta\varphi)$ and $\mu Ci(\theta)$ are the membership functions of the three inputs (ΔT, $\Delta\varphi$, θ) respectively and αi is the i[th] rule weighting factor [25].

5 SIMILATION RESULTS AND DISCUSSION

To test the control strategy effectiveness and robustness, a MATLAB/Simulink simulation is made for a daily solar radiation. The simulated PV water pumping system with FDTC (Fig.3) is composed of 11 PV arrays of 110W connected in series.

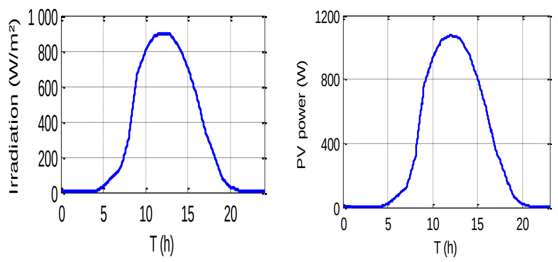

(a) (b)

Figure 5. (a). Irradiance and (b). PV power with Fuzzy MPPT.

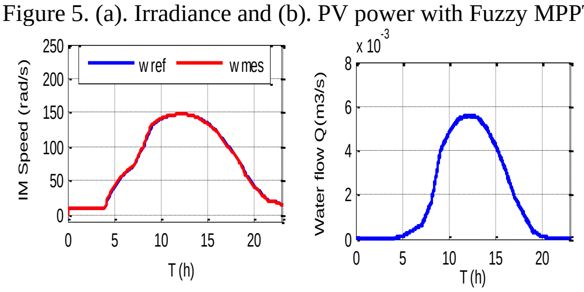

(a) (b)

Figure 6. (a). Moteur speed and (b). Water flow.

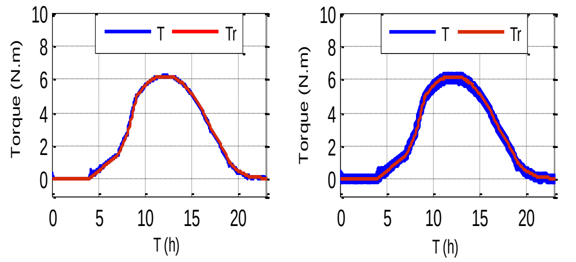

(a). FDTC (b). CDTC

Figure 7. Electromagnetic and resistive torque.

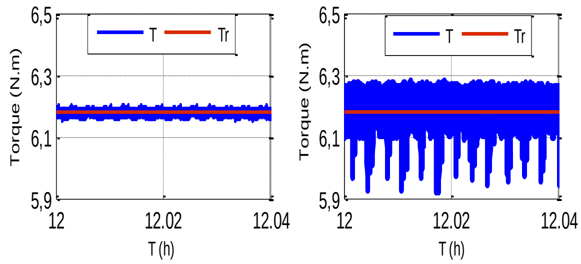

(a). FDTC (b). CDTC

Figure 8. Zoom of Electromagnetic and resistive torque

.

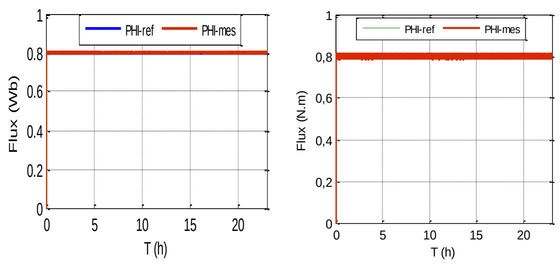

(a). FDTC (b). CDTC

Figure 9. Stator flux response.

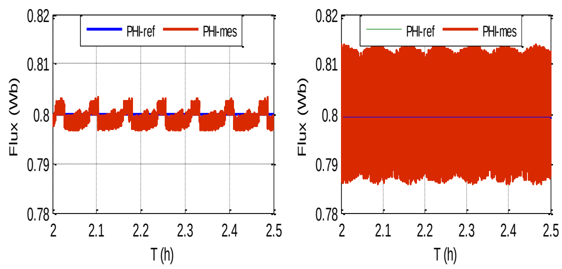

(a). FDTC (b). CDTC

Figure 10. Zoom of Stator flux response.

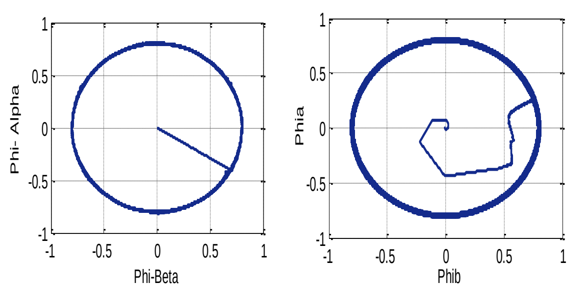

(a). FDTC (b). CDTC

Figure 11. Stator flux trajectory.

The reference flux is φ_{sref} = 0.8Wb. The IM voltage changes as a function of when irradiation. The DC bus voltage is controlled to the reference value of 570V by a PI controller.

The referential speed varies and depends on the extracted PV power. The IM parameters are given in the Appendix. Simulation results show that the proposed FDTC outperforms the CDTC method even under rapidly changing atmospheric conditions.

Figure. 5 shows the irradiation evolution and the PV power. The corresponding IM speed (Fig s.6) tracks perfectly its reference value obtained from the PV power. The water-flow waveform follows the IM speed evolution. The torque response for both control strategies (CDTC and FDTC) is shows in Fig. 7. Comparing the curves, a significant reduction in torque ripples when using FDTC, (Figs. 8).

The stator-flux magnitude is constant and closely follows its reference value (Figs. 9). Zooming those figures shows a better response with fewer ripples when

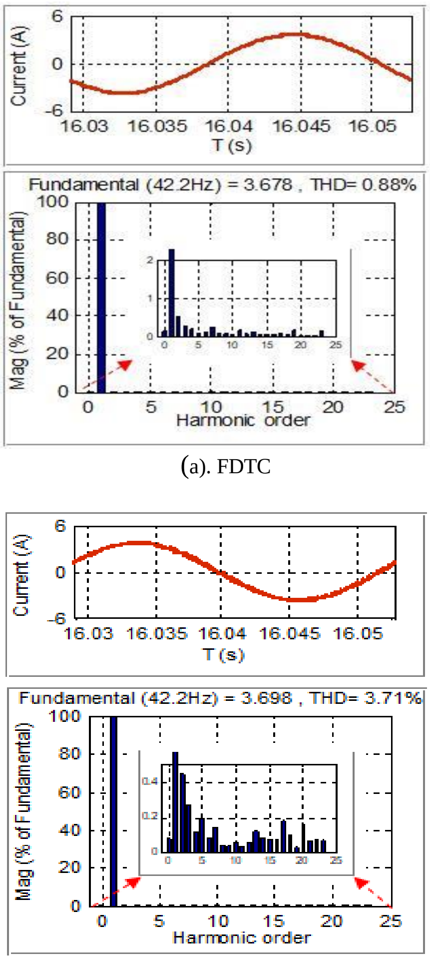

(a). FDTC

(b). CDTC

Figure 12. Zoom of stator current waveform and THD analysis.

comparing FDTC to CDTC (Figs.10). The stator-flux trajectory is circular for both control techniques.

Table 4. Performances analysis of FDTC and CDTC.

Performances	ΔT (N.m)	Δφ (Wb)	THD
CDTC	±0.18	±0.0135	3.71
FDPC	±0.02	±0.0025	0.88
Improvement (%)	**88.89**	**81.48**	**76.28**

Smooth circular path is observed when using FDTC, (Fig. 11).

The stator current waveform is sinusoidal and its THD is 4.72 % and 1.6, respectively.

A comparison between CDTC and FDTC applied to a PV pumping system is made. The resuls presented in Table. 4 show a significant reduction of more than 81% in the flux and EM torque ripples and an improvement in the THD currents of 76% when FDTC is used.

6 Conclusion

The paper proposes an enhancement using a fuzzy switching table applied to an IM driving centrifugal pump in a PV water pumping application. The optimal PV system operation is ensured by a fuzzy logic MPPT controller compared to the traditional method, the presented results show fast and fine tracking regardless of atmospheric conditions. In the proposed FDTC technique, they are no hysteresis controllers and the look-up table replaced by twelve-sector fuzzy inference system. A comparison between the CDTC and FDTC shows simulation results demonstates a significant reduction of 81% in the flux and EM torque ripples and an improvement of 76% in the THD currents when using the proposed method.

The FDTC conserves the robustness, simplicity and high dynamic performance of the CDTC while minimizing its drawbaks related to torque/flux ripple and THD stator current, resulting in less mechanical IM vibrations and reduced acoustic noise.

References

[1] H. Bouzeria, C. Fetha, T. Bahi, I. Abadlia, Z. Layate, S. Lekhchine, “Fuzzy logic space vector direct torque control of pmsm for photovoltaic water pumping system”, Energy Procedia 74, pp. 760 – 771, 2015.

[2] M. Errouha , A. Derouich, S. Motahhir, O. Zamzoum, N. El Ouanjli, A. El Ghzizal, “Optimization and control of water pumping PV systems using fuzzy logic controller”, Energy Reports 5, pp. 853–865, 2019.

[3] S.Lalouni, D.Rekioua, “Control of photovoltaic water pumping system with battery storage”, International Journal of Electrical Engineering & Technology (IJEET), 4 (1), pp. 190-199, 2013.

[4] B.Talbi, F.Krim, T.Rekioua, S.Mekhilef, A.Laib, A.Belaout, 2018. “A high performance control scheme for photovoltaic pumping system under sudden irradiance and load changes” Solar. Energy 159,pp. 353–368, 2018.

[5] M.A.Hannan, J.A.Ali, A.Mohamed, A.Hussain, “Optimization techniques to enhance the performance of induction motor drives: A review” Renew.Sustain. Energy Rev. 81, pp.1611–1626, 2016.

[6] C.M.F.S.Reza, M.D.Islam, S.Mekhilef, “A review of reliable and energy efficient direct torque controlled induction motor drives” Renew. and Sustain Energy Rev. 37, pp.919–932, 2014.

[7] H. Sudheer, SF. Kodad, B .Sarvesh, "Direct torque and flux control of induction machine using fuzzy logic controller", Int.Conference on Advances in Electrical, Electronics, Information, Communication and Bio-Informatics (AEEICB16), pp :1-5, 2016.

[8] W.Ayrir, A. Haddi, "Fuzzy 12 sectors improved direct torque control of a DFIG with stator power factor control strategy", Int. Trans. Electr. Energ. Syst., e12092, 2019. DOI: 10.1002/2050-7038.12092.

[9] N. El Ouanjli, S. Motahhir, A. Derouich, A. El Ghzizal, A. Chebabhi, M. Taoussi, "Improved DTC strategy of doubly fed induction motor using fuzzy logic Controller", Energy Reports 5; pp.271–279, 2019.

[10] H. Merabet Bouluoiha, A. Allali, M. Laouer, A. Tahri, Denaï and A .Draou. "Direct torque control of multilevel SVPWM inverter in variable speed SCIG-based wind energy conversation system" Renewable Energy, 80: pp.140-152, 2015.

[11] M .Mokhtari, SA. Davari "Predictive torque control of DFIG with torque ripple reduction" PECON 2016-2016 IEEE 6th Int. Conf. Power Energy, Conf. Proceeding, pp.763–768, 2017.

[12] A.Benamor, M.T.Benchouia, K.Srairi, M.E.H.Benbouzid, "Electrical power and energy systems a novel rooted tree optimization apply in the high order sliding mode control using super-twisting algorithm based on DTC scheme for DFIG" Electr. Power Energy Syst. 108, pp.293–302, 2019.

[13] R. Chenni, L. Zarour, A. Bouzid and T. Kerbache, "Comparative study of photovoltaic pumping systems using a permanent magnet synchronous motor (PMSM) and an asynchronous motor (ASM)", Rev. Energ. Ren. 9, pp.17 – 28, 2006.

[14] H. Benbouhenni, "Seven-level direct torque control of induction motor based on artificial neural networks with regulation speed using fuzzy PI controller", Iranian Journal of Electrical and Electronic Engineering 01, pp:85-94, 2018.

[15] A.Bourouina, A.Djahbar, A.Chaker, Z. Boudjema, "High order sliding mode direct torque control of a DFIG supplied by a five-level SVPWM inverter for the wind turbine", Elektrotehniški Vestnik, 85(5),pp. 263-270, 2018.

[16] Danduproul Kiran Kumar, G. Tulasi Ram Das, "Performance of fuzzy controller based three level direct torque control fed IPMSM", International Journal of Engineering and Advanced Technology (IJEAT), 8 (3), pp.94-100, 2019.

[17] Tulasi Ram Das Gaddam, Kiran Kumar Danduprolu, "Fuzzy logic controller based performance of SPMSM fed with improved direct torque control", International Journal of Renewable Energy Research, 9(3) pp: 1346-1354, 2019.

[18] N.El Ouanjli, S.Motahhir, A. Derouich, A. El Ghzizal, A. Chebabhi, M. Taoussi, "Improved DTC strategy of doubly fed induction motor using fuzzy logic controller", Energy Reports 5;pp.271–279, 2019.

[19] I.Issad, K.Idjdarene, S. Lalouni, "Direct torque control using space vector modulation of wind pumping system with storage", Rev. Roum. Sci. Techn.– Électrotechn. et Énerg. **63** (4), pp. 397–402, 2018.

[20] S.Krim, S.Gdaim, A. Mtibaa and M. F. Mimouni, Design and implementation of direct torque control based on an intelligent technique of induction motor on FPGA", J Electr Eng Technol. 10, pp. 30-40, 2015.

[21] S. Sina Sebtahmadi, H. Pirasteh, S. Hr. Aghay Kaboli, A. Radan, and S. Mekhilef, "A 12-Sector Space Vector Switching Scheme for Performance Improvement of Matrix-Converter-Based DTC of IM Drive", IEEE Trans. on Power Electronics, vol.30, no. 7, 2015.

[22] S. A. Shaikh Mo, R. Maurya, and N. Gupta, "Modified Switching Table-Based Direct Torque Control of Six-Phase Induction Motor Drive", Electric Power Components and Systems, vol.47, no.11-12, pp.1077-1089. 2019.

[23] S. Lalouni, D. Rekioua, T. Rekioua, E. Matagne, "Fuzzy logic control of stand-alone photovoltaic system with battery storage", Journal of Power Sources, 193, pp.899–907, 2009.

[24] H.Deboucha, S.Lalouni Belaid, "Improved incremental conductance maximum power point tracking algorithm using fuzzy logic controller for photovoltaic system", rev. roum. sci. techn.– electrotechn. et energ., **62** (4), pp. 381–387, 2017

[25] R.Toufouti S.Meziane ,H. Benalla, "Direct torque control for induction motor using intelligent techniques", Journal of Theoretical and Applied Information Technology, 3(3), pp.35-44, 2007.

[26] S. Gdaim, A. Mtibaa, M. F. Mimouni, "Design and experimental implementation of DTC of induction machine based on fuzzy logic control on FPGA", IEEE Trans. on Fuzzy Systems, 23(3) , pp. 644 – 655, 2015.

APPENDIX

Table 5. PV array SM110-24 parameters at STC [23]

Parameter	Value
Maximum power (W)	110
Optimal voltage (V)	35
Optimal current (A)	3.15
Open circuit voltage V_{OC} (V)	43.5
Short circuit current I_{sc} (A)	3.45
Temperaure coefficient of V_{OC} (V/^{0}C)	-0.152
Temperaure coefficient of I_{sc} (A/^{0}C)	0.0014

Table 6. IM parameters [7]

Parameter	Value
Rated power (kW)	1.1
Nominal voltage (V)	400/230
Nominal current (A)	2.6/4.5
Stator resistor (Ω)	7.6
Rotor resistor (Ω)	3.6
Stotor inductance (H)	0.6015
Rotor inductance (H)	0.6015
Mutuel inductance (H)	0.5796
Pairs poles number	2
Inertia moment (Kg.m²)	0.0049

Table 7. Centrifugal pump parameters [13]

Parameter	Value
C_1 (m/(rd/s)²)	4.923 10^{-4}
C_2 (m/(rd/s)(m^3/s)	1.582 10^{-5}
C_3 (m/(m^3/s)²)	-18144

Sofia Lalouni Belaid received her Engineering, M.Sc. and Ph.D. degrees in electrical engineering in 2002, 2005 and 2009 respectively, from the University of Bejaia, Algeria. She is currently a senior lecturer at the Electrical Engineering Department, Faculty of Technology at the same University. Her research activities include application of robust control in photovoltaic, wind and hybrid power systems, electric machine control and power quality.